

## تأثير الشوائب على سلوك تكلسشذرات كربونات الكالسيوم $\text{CaCO}_3$

\*\*\*بريزفيرا جبتا و\*\*ارنب دي و\*شانسال بيزواز

\*قسم هندسة المواد والمعادن، جامعة جادافور، كالكتا، الهند

\*\*قسم هندسة المواد والمعادن، المعهد الهندي للعلوم الهندسية والتقنية، شيبور، هوراج، الهند

### الخلاصة

وجود الشوائب مثل  $\text{MgCO}_3$ ،  $\text{SiO}_2$ ،  $\text{Al}_2\text{O}_3$  يؤثر على سلوك تكلس الحجر الجيري في أفران الجير. وأجريت بعض الأبحاث لدراسة هذا التأثير. تم العثور على الخواص الميكانيكية مثل مؤشر التحطم ومؤشر الكشط ووجد انها تتعرض لتحسين طفيف مع زيادة المحتوى من الشوائب. معدل التكلس يقل تدريجيا مع مرور الوقت قبل تحقيق الإشباع، ويتم تحديد التفاعل الكيميائي بينية كخطوة معدل السيطرة. يتم احتساب طاقة التنشيط من المنحدر من مؤامرة:  $1 - (1 - 0.5)$  مقابل الوقت، حيث  $f$  هو مدى التكلس. اعتمادا على تكوين شذرات، وطاقة التنشيط تتراوح ما بين 155.389 و 178.112 كيلو جول / مول. تم العثور على وجود  $\text{SiO}_2$  و  $\text{Al}_2\text{O}_3$  لرفع طاقة التنشيط على ما يبدو،  $E$ ، في حين وجود  $\text{MgCO}_3$  يقلل من قيمة  $E$ . تم العثور على متوسط الزيادة في طاقة التنشيط على ما يبدو ليكون 2.38 و 1.71 كيلو جول / مول لكل وحدة كتلة٪ زيادة في  $\text{SiO}_2$  و  $\text{Al}_2\text{O}_3$  على التوالي وانخفاض متوسط في طاقة التنشيط على ما يبدو هو 1.40 كيلو جول / مول لكل وحدة كتلة٪ زيادة في  $\text{MgCO}_3$ .

## The effect of impurities on the calcination behaviour of CaCO<sub>3</sub> nuggets

Prithviraj Gupta\*, Arnab De\*\*, Chanchal Biswas\*

\*Dept. of Metallurgical and Material Engineering, Jadavpur University, Kolkata-700032, India

\*\*Dept. of Metallurgy and Materials Engineering, Indian Institute of Engineering Science and Technology, Shibpur, Howrah- 711103, India

\*Corresponding author: prithviraj90metal@gmail.com

### ABSTRACT

The presence of impurities like SiO<sub>2</sub>, Al<sub>2</sub>O<sub>3</sub> and MgCO<sub>3</sub> affects the calcination behaviour of limestone in lime kilns. Some investigations have been carried out to study this effect. The mechanical properties like shatter and abrasion index are found to improve marginally with increasing content of impurities. The rate of calcination gradually reduces with time before attaining saturation, and interfacial chemical reaction is identified as the rate controlling step. Activation energy is calculated from the slope of the plot:  $1-(1-f)^{0.5}$  vs. time, where  $f$  is the extent of calcination. Depending on the composition of nuggets, the activation energy varies between 155.389 and 178.112 kJ/mol. The presence of SiO<sub>2</sub> and Al<sub>2</sub>O<sub>3</sub> is found to raise the apparent activation energy,  $E$ , while the presence of MgCO<sub>3</sub> lowers the value of  $E$ . The average increase in the apparent activation energy is found to be 2.38 and 1.71 kJ/mol per unit mass percent increase in SiO<sub>2</sub> and Al<sub>2</sub>O<sub>3</sub>, respectively and the average decrease in the apparent activation energy is 1.40 kJ/mol per unit mass percent increase in MgCO<sub>3</sub>.

**Keywords:** Activation energy; calcination; impurities; kinetic models; rate-controlling resistance.

### INTRODUCTION

Limestone, a sedimentary rock, is never found in its purest form in nature. In addition to CaCO<sub>3</sub>, it contains impurities like SiO<sub>2</sub>, Al<sub>2</sub>O<sub>3</sub> and MgCO<sub>3</sub>. Calcination, or high temperature decomposition of limestone, that is carried out in lime kilns to produce quicklime, is an important and widely used commercial process. The effect of the presence of impurities on calcination behaviour of limestone has been investigated by a few researchers (Huang & Daugherty, 1987, 1988; Romero-Salvador et al., 1989; García-Calvo et al., 1990). However, the published literature on this topic is still limited.

Calcination is the decomposition of CaCO<sub>3</sub>, where CO<sub>2</sub> gas is liberated, leaving behind CaO (Gupta *et. al.*, 2007).



The standard Gibbs Free Energy for the process can be expressed as  $\Delta G^\circ_r = 177,100 - 158T$  (J/mol) (Gilchrist, 1989), which suggests that the reaction is thermodynamically feasible above 1121

K. However, the reaction rate is extremely slow at such temperatures and much higher temperature is usually employed commercially.

The gas-solid noncatalytic reaction of calcination of limestone encounters various resistances in series. The rate of reaction is often controlled by one of the resistances. Different model equations representing variations of extent of calcinations with time, for various rate controlling regimes is presented in Table 1 (Halikia et al., 2001). For one model, zero order of reaction was considered, while in all others, the reaction order was assumed to be 1.

**Table 1.** Equations for different rate-controlling regimes (Halikia et al., 2001)

Controlling regimes	Functional relationship between extent of fractional conversion, $f$ and time, $t$ $g(f) = k.t$ $f$ – Fractional Conversion $k$ – Apparent rate constant $t$ – Time of reaction
First order phase boundary chemical reaction	$\ln(1-f) = k.t$
Zero order chemical reaction	$f = k.t$
(Interfacial chemical reaction (for cylinder	$(1-f)^{1/2} = k.t$
Diffusion: Ginstling-Brounshtein (GB) equation (for cylinder	$(1-f) \ln(1-f) + f = k.t$
(Diffusion: Jander's equation (for cylinder	$(1-f)^{1/2}]^2 = k.t - 1]$
Nucleation: Avrami-Erofeev equation	$(-\ln(1-f))^{1/n} = k.t$

Ar & Dogu (2001) investigated by thermo gravimetric analysis (TGA) the calcination reaction behaviour of 10 different limestone samples, taken from different regions of Turkey. Shrinking core model with surface reaction rate controlling mechanism was found to be the best model, fitting the experimental data. The activation energies for calcination of various limestone samples were found to be in the range 167-209 kJ/mol.

Okonkwo & Adelifa (2012) studied the calcination kinetics of high calcium type of limestone found in the central region of Nigeria at temperatures 900 °C, 1000 °C, 1060 °C and 1080 °C. Diffusivity and mass transfer coefficient were found to decrease with calcination temperature. 1060 °C was found to be the optimal calcination temperature and lime reactivity was found to improve with decrease in calcination temperature.

Moffat & Walmsley (2006) undertook a fundamental investigation into lime calcination kinetics for the purpose of improving kiln efficiency. A kinetic behaviour diagram was constructed, which was used to explain ways of improving kiln energy efficiency. Experiments, carried out in a laboratory kiln, and later in an industrial kiln, showed 13% increase in energy efficiency and production.

Mu'azu et. al. (2011) investigated the calcination kinetics for Jakura limestone using Power Rate law, for different temperatures between 800°C and 1200°C. It was observed that optimum

conversion time within the temperature range was six hours with maximum conversion of 91.01% achieved at 1200°C. The activation energy for the process was found to be 121.708 kJ/mol.

Fall et al. (2011) demonstrated that microwave-assisted technology directly heated up limestone, leading to the elimination of thermal conduction as the sole mode of heat transfer. Guo et al. (2015) demonstrated that water vapour improved the calcination rates, thus reducing the reaction time. Those influences were stronger for high impurity limestone, which was attributed to greater defects in crystal structure.

Kilic & Anil (2006) studied the effect of limestone characteristics and calcination temperature on the lime quality, produced after reaction. It was found that lime produced at higher calcination temperatures had greater reactivity, which was also highly dependent on the specific surface area, porosity and hydration rate.

Wakefield & Tyner (1950) investigated the calcination of natural limestone with diameter of 0.05 to 0.20 cm at temperatures between 760°C and 927°C. They studied the effect of particle size, calcination temperature and CO<sub>2</sub> concentration on the rates of calcination and developed an equation that empirically represented the data. It indicated that diffusion rate of CO<sub>2</sub> from the particle controlled the calcination rate.

Lindquist et al. (1998) suggested that fluidized beds and suspension calciners were expected to give satisfactory results to fine limestone calcination. The decomposition kinetics of carbonate particles in combustion products was analysed by Batenin et al. (2015) applying the available publications in order to predict the efficiency of reactors for practical use. The thermal decomposition of limestone had been selected as a model reaction for developing an atmospheric open solar reactor by Imhof (2000). In this study, 85% of calcination was obtained for cement raw material and 15% of the solar input was converted into chemical energy (enthalpy). It was shown by James & Richards (1992) that rapid, high temperature calcination would result in a calcined product with relatively large surface area, as desired for sulphur capture.

Romero-Salvador et al. (1989) and García-Calvo *et al.* (1990) observed that the kinetic parameters were strongly affected by small amounts of impurities, though the kinetic model was not affected. The activation energy for calcite containing at least 98.2% of calcium carbonate was 110.5 kJ/mol and was 193.8 kJ/mol for calcite with 99.5% of calcium carbonate. The kinetic model in both cases was a superficial reaction in cylindrical geometry. They reported that low activation energies for calcite decomposition was due to the presence of impurities and/or physical processes, such as sintering. Huang & Daugherty (1987, 1988) found that V<sub>2</sub>O<sub>5</sub> and fly ash inhibited calcination while Al<sub>2</sub>O<sub>3</sub> and CaO had no effect and Li<sub>2</sub>CO<sub>3</sub> accelerated the reaction. Gupta & De (2016) investigated the effect of impurities on the kinetics of calcination of dolomite and the presence of CaCO<sub>3</sub> was found to increase the apparent activation energy, E.

In the present work, nuggets of different compositions were prepared, and the activation energies of decomposition for each composition was calculated from the weight loss method.

## EXPERIMENTAL METHOD

Pure  $\text{CaCO}_3$ ,  $\text{SiO}_2$ ,  $\text{Al}_2\text{O}_3$  and  $\text{MgCO}_3$  were used to prepare the nuggets used in the study, where 3% bentonite and 2% moisture by weight was added to obtain good binding properties. All the raw materials were procured from M/s Quinn India Limited, Kolkata. An electromagnetic stirrer was used to prepare a homogeneous mixture. 15 grams of the mixture was then taken in a cylindrical die (Figure 1), which was placed in a manually operated hydraulic press. A pressure of  $300 \text{ kgf/cm}^2$  was applied. Cylindrical nuggets of predetermined composition and of 30 mm height and 20 mm diameter were taken out of the hydraulic press after ten minutes. The nuggets prepared were then dried at  $110^\circ\text{C}$  for two hours. Mechanical strength of the nuggets was assessed by shatter and abrasion tests.



**Fig. 1.** Die and piston for making nuggets

The nuggets, each with different composition, had identical shapes and approximately identical mass. The nuggets were then placed in an electrically heated tubular furnace (Figure 2), once the desired operating calcination temperature was reached. The furnace consisted of a silicon carbide heating element with a PID temperature controller. The sample was taken in a sample holder of length 82 mm and inner diameter of 33 mm. It was designed such that no air was allowed to enter the system. Four operating calcination temperatures were used: 1173 K, 1273 K, 1373 K and 1473 K. After pre-determined reaction time, i.e., 80 min, 160 min, 240 min, and 320 min, one nugget was taken out, and the loss in weight was measured.



**Fig. 2.** Electrically heated tubular furnace

Extent of calcination,  $f$ , was calculated as a ratio of weight loss to the maximum removable CO<sub>2</sub> mass at various time intervals for the different operating temperatures. The slope of  $g(f)$  vs. time straight line was used in the determination of the factor,  $k$ , the apparent rate constant. The slope of  $\ln k$  vs.  $1/T$  straight line was used to calculate apparent activation energy for the reactions. The same procedure was repeated for all the nuggets, made up of various compositions.

## RESULTS AND DISCUSSION

### Mechanical strength of limestone nuggets

Mechanical properties of the limestone nuggets were determined by abrasion and shatter test. The results for different samples are given in Table 2. It is observed that both abrasion and shatter test improved marginally with the addition of impurities like SiO<sub>2</sub>, Al<sub>2</sub>O<sub>3</sub> and MgCO<sub>3</sub>, though the increase was not significant.

**Table 2.** Composition of the samples and their shatter and abrasion Index

	CaCO <sub>3</sub> (mass percent)	SiO <sub>2</sub> (mass percent)	Al <sub>2</sub> O <sub>3</sub> (mass percent)	MgCO <sub>3</sub> (mass percent)	Shatter Index	Abrasion Index
Sample A	100	0	0	0	78.34	80.35
Sample B	98	2	0	0	79.01	82.38
Sample C	96	4	0	0	79.98	82.47
Sample D	94	6	0	0	79.51	83.14
Sample E	98	0	2	0	78.78	82.96
Sample F	96	0	4	0	79.04	82.29
Sample G	94	0	6	0	78.41	82.48
Sample H	98	0	0	2	78.45	82.96
Sample I	96	0	0	4	78.92	81.75
Sample J	94	0	0	6	79.95	82.33

### Calcination kinetics of pure and doped nuggets of CaCO<sub>3</sub>

The calcination behaviour of pure and doped nuggets of CaCO<sub>3</sub> was studied in detail. It was found that the degree of calcination increased with reaction time and reaction temperature. Also, the rate of calcination reduces gradually with time.

The rate controlling step was identified by kinetic studies.  $g(f)$  vs. time plots (Table 1) were tried out for 6 different rate controlling resistances; (1) First order phase boundary chemical reaction,  $-\ln(1-f) = k.t$ ; (2) Zero order chemical reaction,  $f = k.t$ . (3) Interfacial chemical reaction (for cylinder),  $1-(1-f)^{1/2} = k.t$ ; (4) Diffusion: Ginstling-Brounshtein (GB) equation (for cylinder),  $(1-f) \ln(1-f) + f = k.t$ ; (5) Diffusion: Jander's equation (for cylinder),  $[1 - (1-f)^{1/2}]^2 = k.t$ ; (6) Nucleation: Avrami-Erofeev equation,  $[-\ln(1-f)]^{1/n} = k.t$ . For Avrami-Erofeev equation, the value of  $n$  was chosen to be 2. For one model, zero order of reaction was considered, while in all others, the reaction order was assumed to be 1. It was observed that the R<sup>2</sup> values for many of the rate

controlling resistances were nearly 1 at low temperatures as the extent of reaction is low; but at high temperatures, R2 values were much less than 1, indicating non-linearity (Table 3). Only for interfacial chemical reaction control, the R<sup>2</sup> values are nearly equal to 1 at all temperatures. The g(f) vs. t plots for 6 different rate controlling resistances at 1473 K are presented in Figure 3, which indicated that only the interfacial chemical reaction control plot shows linearity, while others were significantly non-linear. After comparing the nature of fit with the linear relationship of g(f) vs. t in terms of the values of R<sup>2</sup> for different models for all samples at all temperatures, it is concluded that interfacial chemical reaction exhibited highest R<sup>2</sup> value and, hence, is the rate-controlling resistance. The rate-controlling resistance was not found to be affected by the presence of impurities. It may be mentioned that a similar rate-controlling resistance was identified by García-Calvo *et al.* (1990) and Halikia *et al.* (2001) for decomposition of CaCO<sub>3</sub>.

**Table 3.** Regression coefficient (R<sup>2</sup>) for fitting different kinetic models  $g(f) = k.t$

<b>g(f) / Temperature (K) →</b>	1173	1273	1373	1473
$1 - [(1-f)^{0.5}]$	0.9953	0.9968	0.9877	0.9936
$-\ln(1-f)$	0.9955	0.9938	0.9828	0.9268
$(1-f) \ln(1-f) + f$	0.9034	0.8575	0.8811	0.9473
$[1 - (1-f)^{1/2}]^2$	0.9027	0.8500	0.8697	0.8982
$[-\ln(1-f)]^{0.5}$	0.8483	0.8810	0.8839	0.9698
$f$	0.9950	0.9977	0.9842	0.9052

The apparent reaction rate constant, k, was obtained from the slope of the plot  $1 - (1-f)^{0.5}$  vs. time at all temperatures.

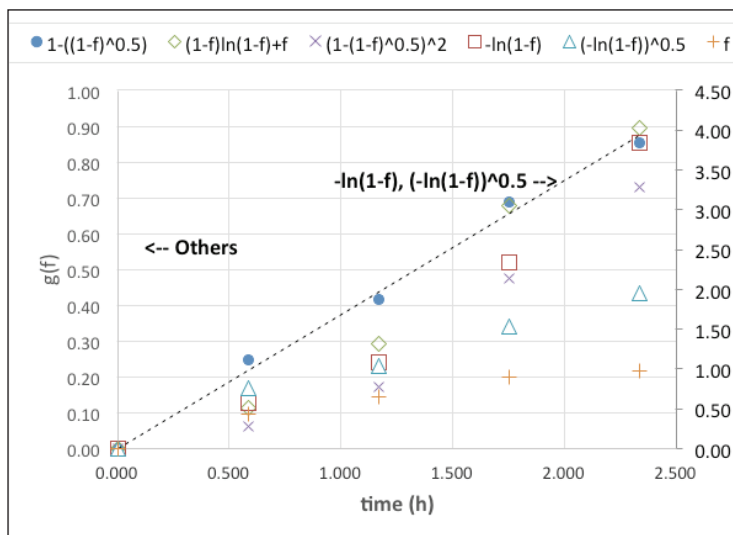


**Fig. 3.** The plot of g(f) vs. time for calcination of pure CaCO<sub>3</sub> nuggets at 1473 K

The apparent activation energy,  $E$ , was determined from the slope of the plot  $\ln k$  vs.  $1/T$  for nuggets of different composition and is summarised in Table 4. Only a sample plot for pure  $\text{CaCO}_3$  is shown in Figure 4. The apparent activation energy was found to vary between 155.389 and 178.112 kJ/mole depending on the composition of the nugget. The activation energy values are comparable with that determined by Ar & Dogu (2001) and Mu'azu *et al.* (2011) at 167-209 kJ/mol and 121.708 kJ/mol respectively. The  $R^2$  values of the linear fitting of the plot  $\ln k$  vs.  $1/T$  were found to be fairly satisfactory (Table 4).

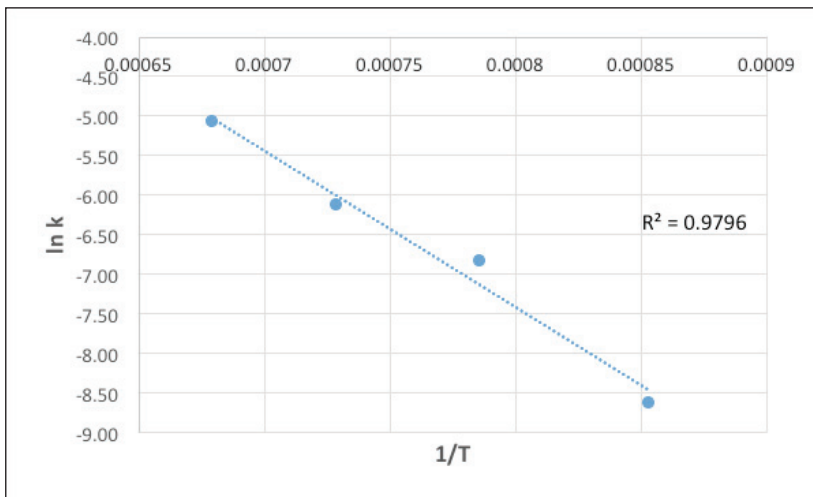


**Fig. 4.** The plot of  $\ln k$  vs.  $1/T$  for calcination of pure  $\text{CaCO}_3$  nuggets

**Table 4.** Effect of Al<sub>2</sub>O<sub>3</sub> mass percent, SiO<sub>2</sub> mass percent and MgCO<sub>3</sub> mass percent on activation energy, E (kJ/mol)

Sample	1/T	ln k	E	R <sup>2</sup>
Pure CaCO <sub>3</sub>	0.000853	-8.61	164.135	0.9429
	0.000786	-6.82		
	0.000728	-6.12		
	0.000679	-5.06		
2% Al <sub>2</sub> O <sub>3</sub>	0.000853	-8.75	168.6827	0.9301
	0.000786	-6.76		
	0.000728	-6.16		
	0.000679	-5.07		
4% Al <sub>2</sub> O <sub>3</sub>	0.000853	-8.84	173.0975	0.8587
	0.000786	-6.83		
	0.000728	-6.24		
	0.000679	-5.05		
6% Al <sub>2</sub> O <sub>3</sub>	0.000853	-9.03	174.0952	0.963
	0.000786	-6.62		
	0.000728	-6.45		
	0.000679	-5.09		
2% SiO <sub>2</sub>	0.000853	-8.64	166.2052	0.963
	0.000786	-8.22		
	0.000728	-6.58		
	0.000679	-5.27		
4% SiO <sub>2</sub>	0.000853	-8.74	171.8836	0.9192
	0.000786	-7.99		
	0.000728	-6.39		
	0.000679	-5.25		
6% SiO <sub>2</sub>	0.000853	-8.59	178.1108	0.9518
	0.000786	-8.38		
	0.000728	-6.28		
	0.000679	-5.09		
2% MgCO <sub>3</sub>	0.000853	-8.55	158.6062	0.996
	0.000786	-7.15		
	0.000728	-6.41		
	0.000679	-5.11		
4% MgCO <sub>3</sub>	0.000853	-8.63	156.8187	0.9766
	0.000786	-6.72		
	0.000728	-6.10		
	0.000679	-5.24		
6% MgCO <sub>3</sub>	0.000853	-8.67	155.3887	0.963
	0.000786	-6.62		
	0.000728	-6.20		
	0.000679	-5.25		

The presence of Al<sub>2</sub>O<sub>3</sub> is found to increase the apparent activation energy (Table 4). The activation energy is nearly linear with the mass percent of Al<sub>2</sub>O<sub>3</sub> (Figure 5) and the average increase in the apparent activation energy is 1.715 kJ/mol per unit mass percent increase in Al<sub>2</sub>O<sub>3</sub>. The presence of SiO<sub>2</sub> is also found to raise the apparent activation energy (Table 4). The average increase in the apparent activation energy is 2.380 kJ/mol per unit mass percent increase in SiO<sub>2</sub> (Figure 6). The presence of MgCO<sub>3</sub> is found to decrease the apparent activation energy (Table 4) and the average decrease in the apparent activation energy is 1.401 kJ/mol per unit mass percent increase in MgCO<sub>3</sub> (Figure 7).

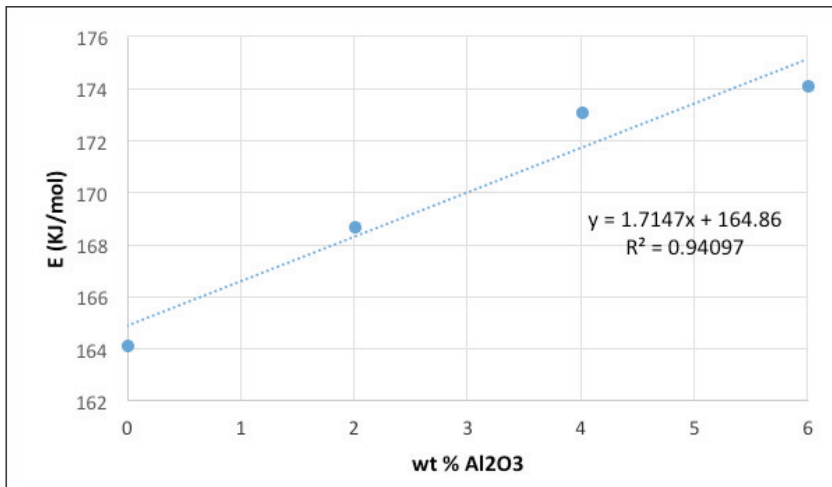


**Fig. 5.** The plot of E vs. Al<sub>2</sub>O<sub>3</sub> mass percent in the CaCO<sub>3</sub> nuggets

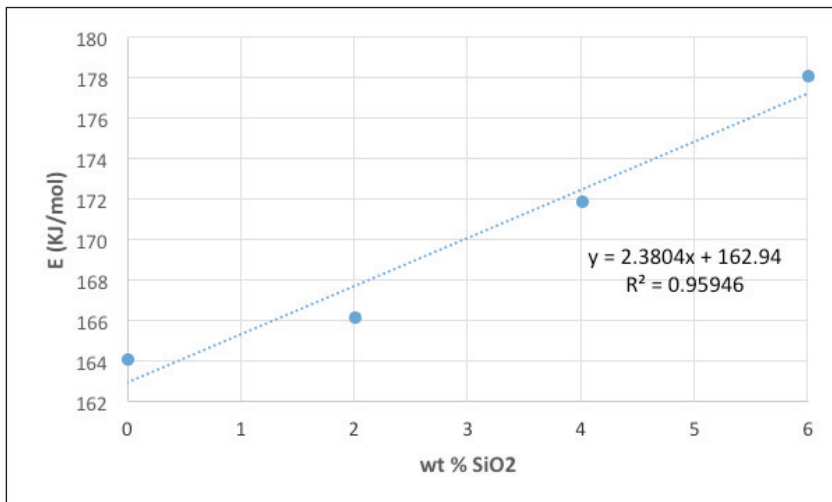


**Fig. 6.** The plot of E vs. SiO<sub>2</sub> mass percent in the CaCO<sub>3</sub> nuggets

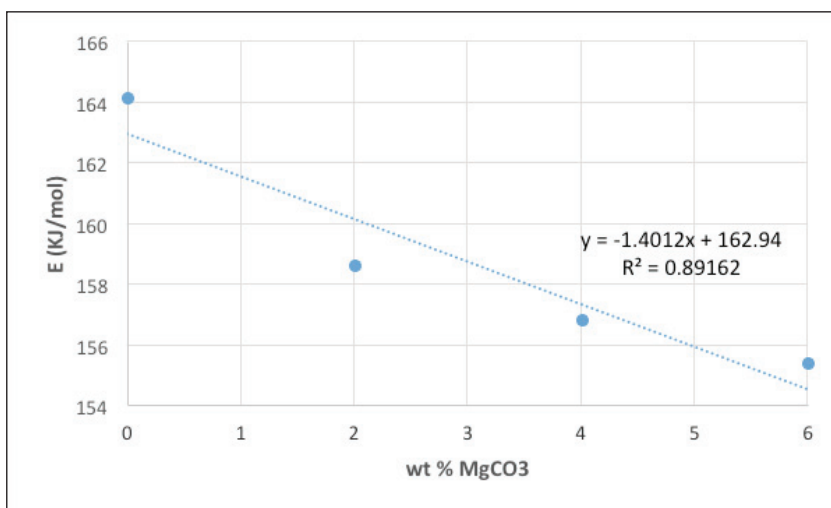


**Fig. 7.** The plot of E vs. MgCO<sub>3</sub> mass percent in the CaCO<sub>3</sub> nuggets

## CONCLUSIONS

1. The mechanical properties like shatter index and abrasion index are found to improve marginally with increased content of the gangue materials. However, the improvement is too insignificant to draw a sharp conclusion.
2. First order interfacial chemical reaction is found to control the overall rate of reaction.
3. Apparent activation energy varies between 155.389 and 178.112 kJ/mole, depending on nugget composition.
4. The presence of Al<sub>2</sub>O<sub>3</sub> and SiO<sub>2</sub> increases the activation energy, while the presence of MgCO<sub>3</sub> lowers its value.

## REFERENCES

- Ar, I & Dogu, G. 2001.** Calcination kinetics of high purity limestone. *The Chemical Engineering Journal*, **83**(2):131-7
- Batenin, V. M., Kovbasyuk, V. I., Kretova, L. G. & Medvedev, Y. V. 2015.** Dust reactor for limestone calcination. *High Temperature*. Pleiades Publishing, **53**(2):289-98
- García-Calvo E., Arranz, M. A. & Letón P. 1990.** Effects of impurities in the kinetics of calcite decomposition. *Thermochimica Acta*, **170**:7-11.
- Fall, M., Esquenazi, G., Allan, S. & Shulman, H. & Ceralink Inc. 2011.** Rapid limestone calcination using Microwave Assist Technology. 35th International Conference & Exposition on Advanced Ceramics and Composites. ICACC-S8-023-2011, Daytona Beach, Florida, USA.
- Gilchrist, J.D. 1989.** *Extraction metallurgy* (3rd ed.). Oxford: Pergamon Press. p. 145. ISBN0-08-036612-0.
- Guo, S., Wang, H., Liu, D., Yang, L., Wei, X. & Wu, S. 2015.** Understanding the impacts of impurities and water vapor on limestone calcination in a laboratory-scale fluidized bed. *Energy Fuels*, **29**(11):7572-83

- Gupta, P. & De, A. 2016.** The Effect of composition on the decomposition behaviour of dolomite nuggets. *Imperial Journal of Interdisciplinary Research*, **2**(3):321-4
- Gupta, S.K., Ramakrishnan, A. & Hung, Y.T. 2007.** *Advanced physicochemical treatment technologies.* Springer-Verlag, Berlin: 611-33
- Halikia,I., Zoumpoulakis, L., Christodoulou, E. & Prattis, D. 2001.**The European Journal of mineral processing and environmental protection. Kinetic study of the thermal decomposition of calcium carbonate by isothermal methods of analysis. *The European Journal of Mineral Processing and Environmental Protection*, **1**(2):89-102.
- Huang, J. M. & Daugherty K. E. 1987.** Lithium carbonate enhancement of the calcination of calcium carbonate: proposed extended-shell model. *ThermochimicaActa*, **118**:135–41.
- Huang, J. M. & Daugherty K. E. 1988.** Inhibition of the calcination of calcium carbonate. *Thermochimica Acta*, **130**:173–6.
- Imhof, A. 2000.** Calcination of limestone in a solar reactor. *ZKG International*, **53**: 504-9
- James, R. E. & Richards, G. A. 1992.** Limestone calcination during pulsating combustion. 1992. Atomic Energy Commission USA -Reports- 285. Coal-fueled heat engines, advanced pressurized fluidized-bed combustion and gas stream clean up systems contractors review meeting
- Kilic, O. & Anil, M. 2006.** Effects of limestone characteristic properties and calcination temperature on lime quality. *Asian Journal of Chemistry*, **18**(1):655-66
- Lindquist, W., Prokesch, M. & Smith, D. 1998.** Calcination of limestone fines. *World Cement.Palladian publications*, **29**(3):8-18
- Moffat, W. & Walmsley, M.R.W. 2006.** Understanding lime calcination kinetics for energy cost reduction. 59thAppita Conference, Auckland, New Zealand, 16-19 May 2006.
- Mu'azu, K., Abdullahi, M. & Akusu, A.S. 2011.** Kinetic study of calcination of jakura limestone using power rate law model. *Nigerian Journal of Basic and Applied Sciences*, **19**(1): 116-20.
- Okonkwo, P.C. & Adelifa, S.S. 2012.**The Kinetics of calcination of high calcium limestone. *International Journal of Engineering Science and Technology*, **4**(2):391-400.
- Romero-Salvador, A., García-Calvo, E. & Benitez Aparicio, C.1989.** Effects of sample weight, particle size, purge gas and crystalline structure on the observed kinetic parameters of calcium carbonate decomposition. *Thermochimica Acta*, **143**:339-45.
- Wakefield, A. & Tyner, M. 1950.** Low Temperature calcination rates of limestone. *Industrial & Engineering Chemistry. American Chemical Society*, **42**(10):2117-21.